Image Contrast Enhancement Based on Equalization of Edge Histograms

Iyad F. Jafar and Khalid A. Darabkh

Abstract— **Image contrast enhancement finds its place in many imaging applications. Unsharp masking is a classical tool for image contrast sharpening. The basic idea in this method relies on emphasizing the edge information in the image by adding a scaled version of the high frequency content of image to the original image. Despite its simplicity and effectiveness, unsharp masking suffers from noise amplification, edge ringing artifacts, and the need for specifying the scaling factor. In this paper, we propose a novel technique for scaling the edge information in order to achieve higher levels of enhancement with lower levels of noise amplification and ringing artifacts. The proposed technique utilizes an adapted version of the popular histogram equalization technique to amplify the edge information automatically and adaptively. Experimental evaluation proves the validity of the proposed technique in producing better contrasted images, qualitatively and quantitatively.**

Index Terms— **Contrast enhancement, histogram equalization, image erosion, Laplacian mask, ringing artifacts**

I. INTRODUCTION

THE availability of multimedia and communication systems has increased the interest in image data in many fields such as astronomy, remote sensing, medical sciences, science of materials, and biology. Regardless of the field, the quality of the captured images might be degraded for one or more reason such as malfunctioning issues in the imaging device and/or insufficient lighting and presence of noise in the environment. The level of degradation could be high enough to affect the usefulness of these images. In such occasions, image enhancement [1,2] and denoising [3,4] algorithms techniques come into action, where the degraded images are processed to make them suitable for human viewers or machine vision applications. Although the research in image enhancement techniques has been around for a while, the area is still attracting many researchers due to the subjectivity in evaluating the quality of the processed images and the emergence of new applications for digital images. Actually, the problem of image enhancement is not a trivial task since each image has its own characteristics, in addition to the fact that different image applications demand different enhancement requirements. Thus, it is hard to find a universal enhancement technique that would satisfy such diverse requirements. In fact this justifies the presence of a plenty of techniques in the literature.

In general, image enhancement techniques can be grouped into two main categories; direct and indirect techniques [1,2]. In the indirect approaches, the intensities or color channels are modified by means of some transformation function such that the dynamic range of the display device is fully utilized and the image details are more distinct. Contrast stretching using linear and nonlinear functions [5,6], histogram equalization and specification [7]-[11], iterative histogram thinning [12], graylevel grouping [13] and fuzzy contrast intensification [14] are examples of the indirect enhancement techniques. Generally, indirect contrast enhancement techniques are successful in improving the global quality of the image. However, they usually fail to enhance local details.

On the contrary, direct enhancement techniques attempt to improve the image contrast by manipulating some local contrast measure that is usually related to the edge information and local statistics in the image. The contrast measure is typically selected based on prior knowledge of the imaging application. In [15], Matz and Figueriedo proposed a contrast enhancement technique that stretches the intensity values based over the Munsell's scale [16] intervals based on an optimal transformation function and the mean edge gray values contrast measure proposed by Beghdadi *et al.* [17]. Performance evaluation of this technique shows its ability in contrast sharpening. However, it results in noise amplification. This is because the transformation function depends only on the minimum and maximum intensity values of the intensity intervals defined in the Munsell's scale, out of which are some wide intervals. This may result in excessive stretching and accumulation of the intensities near the endpoints of the intervals, which leads to noise amplification. Hanmandlu and Jha proposed a novel enhancement method that is based on fuzzifying the image using a Gaussian membership function and then applying a global contrast intensification operator [18].

The technique proposed by Cheng *et al.* [19] builds on the techniques in [15] and [17], however, a set of four homogeneity measures are used to compute the local contrast at each pixel. Additionally, the technique automatically specifies the parameters of the contrast modification function. Another technique in this category is presented in [20] where contrast enhancement by using the intensity-pair distribution which reflects both global and local information of the image content. Based on this distribution a set of expansion and anti-expansion forces are computed and used to define a transformation function that is used to modify pixel intensities.

Among the direct enhancement techniques is the unsharp masking [21]. Basically, this technique relies on

Manuscript received December 28, 2010; revised May 26, 2011.
I. F. Jafar is with the Department of Computer Engineering at The University of Jordan, Amman 11942, Jordan; phone: +962-6-535500; fax: +962-6-5300813; e-mail: iyad.jafar@ju.edu.jo.
K. A. Darabkh is with the Department of Computer Engineering at The University of Jordan, Amman 11942, Jordan; e-mail: k.darabkeh@ju.edu.jo.

(Advance online publication: 24 August 2011)

emphasizing discontinuities in the image based on the fact that the human visual system is sensitive to intensity transitions. Thus, emphasizing discontinuities associated with intensity transitions is expected to improve the image contrast. The enhanced image *g(x,y)* in unsharp masking is obtained by

$$g(x,y) = f(x,y) + \alpha E(x,y) \quad (1)$$

where *f(x,y)* is the original image, *E(x,y)* is the edge image obtained by convolving the original image with a highpass filter mask such as the Laplacian [1,2], and *α* is real scaling factor that is greater than 1. Despite its simplicity and effectiveness in improving the image contrast and sharpness, many complications arise when using unsharp masking for contrast enhancement. First, the edge image usually contains the noise information in the image in addition to the edge information. This leads to amplification of the noise that exists in the image after enhancement, especially in smooth regions. Second, the Laplacian response for many pixels in the image has relatively high positive or low negative values, especially in edge and near-edge regions. Consequently, this may lead to overshooting or undershooting the pixels' intensity values in the output image after addition, thus out of range values. The visual effect of this is what is known as halo or ringing artifacts. Finally, the level of enhancement obtained using unsharp masking depends on manual specification of the scaling factor *α*. Sharper images can be obtained by using large values for *α*; however, this increases the severity of ringing artifacts and noise amplification.

To address the problem of ringing artifacts, the authors in [22,23] suggested making the scale factor variable and inversely proportional to the local standard deviation of the pixel's neighborhood. Although ringing is reduced in these techniques, noise amplification is inevitable since smooth regions are characterized with low standard deviation values. Chang *et al.* [24] proposed a technique to specify the scale factor of the edge image by using a nonlinear contrast gain function that is determined by using a transformation between the local standard deviation histogram and a desired histogram that is derived by extending Hunt's image model. The proposed function produces better results in terms of enhanced image quality and reduced ringing and noise amplification. However, the method is iterative in nature and requires user interaction to specify three different parameters in order to design the suitable contrast gain function.

In this paper, we propose a new contrast enhancement technique that builds on the classical unsharp masking technique and the same time attempts to address its problems. The proposed technique relies on processing the histogram of the edge information and K-means clustering such that: 1) the edge information of noisy pixels is not scaled, 2) the scale factor is specified adaptively and is determined by performing histogram equalization on the edge histogram, 3) the edge information computed using the Laplacian operator is weighted by the pixel intensity values to reduce overshooting and undershooting problems. Additionally, the proposed technique employs a filtering step on the scaled edge image for further reduction of noise amplification and ringing artifacts. The filtering step exploits the use of a different filter mask to compute the edge information instead of the Laplacian, in addition to the morphological erosion operation for edge thinning and removal of isolated noise pixels. The remaining of this paper is organized as follows. In Section II, the proposed technique details and justifications are presented. Experimental enhancement results of the proposed technique are presented in Section III. Finally, the paper is concluded in Section IV.

II. Proposed Technique

A. The Basic Technique

The proposed enhancement technique in this paper is basically based on the unsharp masking technique. However, in order to accommodate for the problem of specifying the scale factor *α* automatically and adaptively, the histogram equalization technique is applied on the histogram of edge image. Histogram equalization is a popular indirect enhancement technique that attempts to redistribute the image intensities over the entire dynamic range by transforming the image histogram into a flat one [1,2]. The function that achieves such transformation is basically

$$T(k) = (L_{\max} - L_{\min})\left(\sum_{i=0}^{k} h(i)\right) + L_{\min},\ k \in \left[L_{\min}, L_{\max}\right] \quad (2)$$

wher *h(i)* is the normalized image intensity histogram, and L_{min} and L_{max} are the minimum and maximum of the intensity dynamic range. Using this function has the effect of stretching the histogram bins toward the two ends of the dynamic range, which is equivalent of scaling the intensity values adaptively. An important observation regarding this function is its simplicity and dependence on the image attributes only.

Based on this argument, the proposed technique in this paper employs the histogram equalization technique to the histogram of the edge image before it is added to the original image. This operation is essentially equivalent to multiplying the edge values by a different scale factor based on the shape of the transformation function obtained using the histogram equalization. Nonetheless, histogram equalization cannot be applied on the edge image in a straight forward manner due to some typical properties of the Laplacian edge image. Figures 1(a), 1(b), and 1(c), show the original image *Peppers,* an example of Laplacian mask, and the corresponding absolute edge image, respectively. Two important observations can be made from this edge image. First, it is obvious how this image has large values for pixels that represent edges and low or zero values for pixels in smooth regions. Second, the double-edge effect is clearly noticeable due to the presence of negative and positive edges which is an inherent property of the Laplacian operator [1,2].

These observations can be also identified by looking at the quantized histogram of the edge information of the *Peppers* image as shown in Figure 1(d). Looking at the edge histogram, we can see how it peaks near zero with most of its large bins located near the origin. Actually, these bins include pixels in pure smooth regions or regions with relatively small intensity variations. For the remaining bins, we can see that they have lower counts and they are centered on lower negative values or higher positive values. Typically, these bins usually correspond to true edge pixels.

(a)

-0.5	-2	-0.5	
-2	10	-2	x1/3
-0.5	-2	-0.5	

(b)

(c)

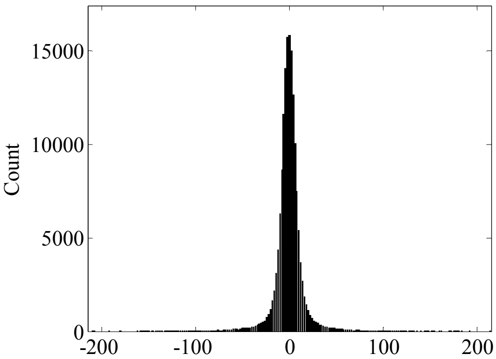

(d)

Fig. 1. Illustration of Laplacian edge response and its properties (a) original image *Peppers* (b) a Laplacian mask example (c) edge image computed using the Laplacian mask (d) edge histogram.

If histogram equalization is applied on the edge histogram over [E_{min} E_{max}], where E_{min} and E_{min} are the minimum and maximum edge values in the image, respectively, then the corresponding transformation function *T(E)* shown in Figure 2(a) is obtained according to (2), where *h(i)* in this case is the normalized histogram of the edge image and *i* is the quantized edge value. This transformation function suggests that bins centered on negative values are excessively pushed toward the minimum edge value E_{min} while bins centered on positive values are excessively pushed toward the maximum edge value E_{max} without any special treatment to the bins

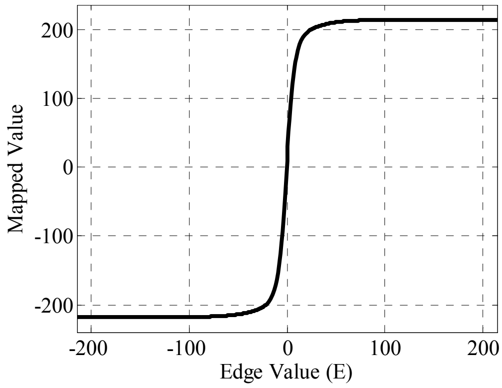

(a)

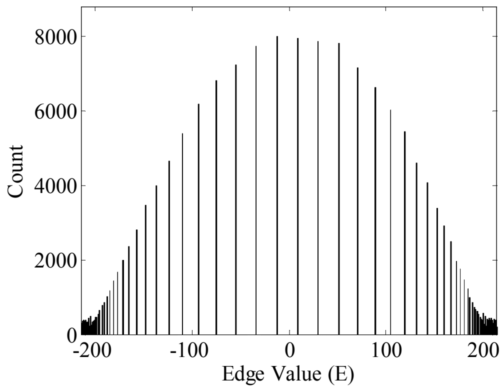

(b)

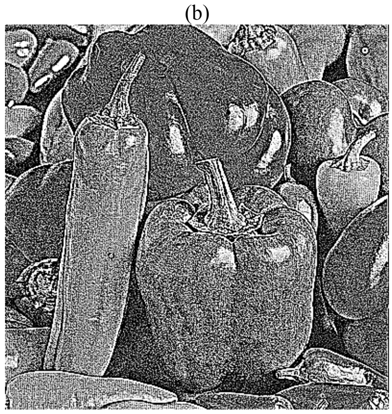

(c)

Fig. 2. Illustration of the basic enhancement technique (a) Transformation function derived from the whole edge histogram (b) Edge histogram after applying the transformation function (c) Enhanced image.

that include noisy pixels, and the overshooting and undershooting of edge values. The effect of this behavior is clearly shown in Figure 2(b) which shows the histogram of the equalized edge image that is characterized with higher contrast, but with severe noise amplification and excessive emphasis of true edge content, or ringing artifacts, as shown in Figure 2(c). In fact, this is a typical example that shows how histogram equalization technique fails when the processed histogram has large bins, which are always present in edge images since the true edge content usually has small contribution in the overall number of pixels in the image. Thus, this inhibits histogram equalization in its basic form to be suitable for the proposed technique.

In the following subsections, the details of adapting the histogram equalization technique to cope for these problems are presented. First, the technique is adapted before the edge image is scaled. Then, a filtering operation for the scaled edge image is proposed to aid the process of reducing noise amplification and ringing artifacts.

B. Adaptation of the Basic Technique

B.1. Pre-scaling Adaptation

Based on the previous discussion, if the edge image is to be scaled automatically, then this should be done carefully such that: 1) edge values that correspond to true edge pixels are not excessively pushed toward the two ends edge dynamic range to reduce edge ringing artifacts, 2) bins that correspond to smooth regions are excluded to avoid noise amplification. Accordingly, scaling the edge image using histogram equalization should comply with these two requirements. In the proposed technique, these problems are addressed according to the following.

Regarding edge ringing artifacts, they are inevitable when unsharp masking is used due to the fact that the Laplacian response suffers from overshooting and undershooting problems, especially when the edge scale factor is high. In other words, the Laplacian may have very high positive or very low negative values for some pixels in the image, specifically, edge pixels. For pixels with high intensity values and high positive Laplacian response, the values of these pixels in the enhanced image could be greater than L_{max} after adding the edge image to the original image. The same argument is true for pixels with low intensity values and low negative edge values. In this case, the intensity values in the output image for these pixels could be lower than L_{min}. Such behavior results in over-emphasizing the edge pixels. As a first step in dealing with this problem in the proposed technique, a weighted edge image is used instead of the edge image $E(x,y)$ in the enhancement process. The weighted edge image is obtained by

$$E^{w}(x,y)=\begin{cases} E(x,y)\ \dfrac{f(x,y)}{L_{\max}} & ,E(x,y)<0 \\ E(x,y)\ \dfrac{L_{\max}-f(x,y)}{L_{\max}} & ,E(x,y)>0 \end{cases} \tag{3}$$

The argument behind scaling the edge image using (3) is that for pixels with positive Laplacian response, the edge value is weighted by a factor that reflects the intensity level of the pixel, such that the closer the intensity to L_{max} , the lower the weighting factor. Therefore, when the edge information is added to the intensity of the pixel, the possibility of exceeding L_{max} is reduced. Similarly, for pixels with negative Laplacian response, the edge values are scaled such that the closer the intensity to L_{min}, the lower the weighting factor. Again, this reduces the possibility of getting values lower than L_{min}.

In order to address the issue of specifying the scaling factor α of the edge image adaptively and automatically, the basic technique applies the histogram equalization technique on the edge histogram. However, such approach is not effective as it doesn't provide special treatment for noise pixels and it may result in over stretching the edge values, which may lead to noise amplification and ringing artifacts. Actually, the overstretching problem is also encountered when histogram equalization is applied to the intensity values and many approaches have been proposed to deal with this problem [25]-[28]. The basic idea in some of these approaches is to divide the dynamic range of the image into two or more sub-range and then apply the histogram equalization technique on the sub-histograms independently.

TABLE I
VALUES USED TO EXTRACT THE EDGE SUB-HISTOGRAMS

Sub-histogram	Lower Value	Upper Value
$h_1(i)$	$E^{w}_{\min}$	δ_1
$h_2(i)$	δ_1+1	δ_2
$h_3(i)$	δ_2+1	δ_3
$h_4(i)$	δ_3+1	δ_4
$h_5(i)$	δ_4+1	$E^{w}_{\max}$

On overall, such approach limits the stretching of the intensity bins, thus reducing the problems related to overstretching. Consequently, the second adaptation to the basic technique borrows the concept of divided histogram equalization to overcome overstretching problems. Another advantage of working with divided edge histograms is that the edge bins that correspond to noise pixels can be excluded from the equalization operation to reduce noise amplification.

In the proposed technique, the edge histogram is divided into five sub-histograms $h_1(i)$, $h_2(i)$, $h_3(i)$, $h_4(i)$, and $h_5(i)$ using four thresholds δ_1, δ_2, δ_3, and δ_4 such that

$$E^{w}_{\min} < \delta_1 < \delta_2 < 0 \tag{4}$$

and

$$0 < \delta_3 < \delta_4 < E^{w}_{\max} \tag{5}$$

with $E^{w}_{\min}$ and $E^{w}_{\max}$ being the minimum and maximum values of the weighted edge image. The five sub-histograms essentially include a subset of the bins from the full edge histogram $h(i)$ over different ranges using the four thresholds as given in Table I. Effectively, the thresholds δ_2 and δ_3, are used to identify the bins that correspond to pixels in smooth regions from the bins of true negative and positive edges. These bins are included in the $h_3(i)$ sub-histogram and are expected to be left unchanged when the edge image is scaled. This should have the effect of reducing noise amplification. The thresholds δ_1 and δ_4 are used to split each of the true negative and positive edge bins into two groups. The first group includes bins with moderate edge values included in the $h_2(i)$ and $h_4(i)$ sub-histograms, while the second group has the bins with high edge values included in the $h_1(i)$ and $h_5(i)$ sub-histograms. This splitting has two roles. First, it limits the stretching of the true edge bins toward the two ends of the histogram, thus reducing ringing artifacts, especially for moderate edge values. Second, if some noise pixels that are supposed to be in $h_3(i)$ are mistakenly included in $h_2(i)$ and $h_4(i)$ sub-histograms, then the splitting of the true edge values limits their amplification.

According to this division, scaling the edge image proceeds by excluding the sub-histogram $h_3(i)$ and manipulating the edge values of the remaining sub-histograms through computing the transformation function for each sub-histogram using equation (2) with L_{min} and L_{max} being the values specified to extract each sub-histogram as given in Table I. The scaled edge image $E^{w}_{scaled}(x,y)$ is computed from the weighted edge image $E^{w}(x,y)$ by replacing the edge value for each pixel with the value computed using the corresponding transformation function based on the sub-range it belongs to. The enhanced image

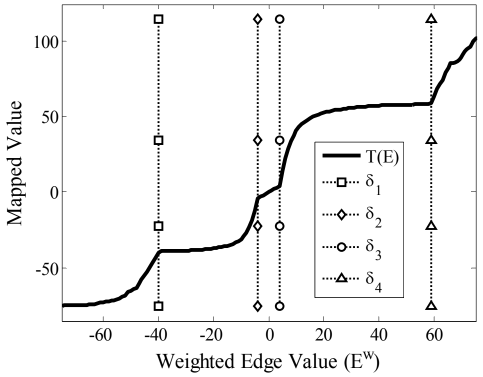

(a)

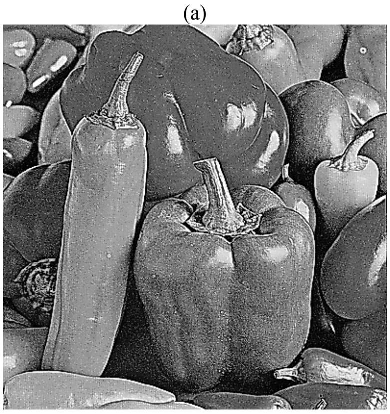

(b)

Fig. 3. Illustration of the effect of pre-scaling adaptation on the basic enhancement technique (a) Combined transformation function (b) Enhanced image.

g(x,y) according to the unsharp masking technique is then computed by adding the scaled image back to the original image using

$$g(x,y) = f(x,y) + E^{w}_{Scaled}(x,y) \tag{6}$$

The combined transformation function for the *Peppers* image using certain values for the four thresholds and the enhanced image are shown in Figure 3(a). Examining this transformation function and the equalized histogram, it is clear how the division of the edge histogram has limited the stretching of the true edge bins to be within a sub-range of the full range of edge values while excluding the bins that represent noise when compared to the transformation function computed by equalizing the entire edge image as shown in Figure 2(a). Actually, such behavior produces a better contrasted image, as shown in Figure 3(b), with less noise amplification and ringing artifacts when compared to the image in Figure 2(c).

B.2. Post-scaling Adaptation

Examining the image produced by the proposed technique in Figure 3(b), it is obvious how the contrast has been significantly increased. However, a closer look into the image reveals that some of the smooth regions have acquired some noise amplification and some of the edges and their neighboring regions appear too bright or too dark (ringing artifacts). Actually, these two problems are imposed by the nature of the Laplacian operator which gives larger weight to the center pixel as shown in the Laplacian mask given in Figure 1(b). This implies that for pixels with relatively high noise levels and those in the regions near the edges, the Laplacian response is relatively high and is not excluded when the K-means clustering is applied. Consequently, when the edge image is added back to the original image, this would result in emphasizing high- level noise pixels and pixels in the regions around the edges. In fact, these problems are more critical in the proposed technique since the edge image is scaled, which increases the severity of the problems.

A simple approach to reduce the effect of noise in the Laplacian edge image is to compute the Laplacian image from a smoothed version of the original image. However, applying the technique using the smoothed Laplacian edge image produces less contrasted image since the edge response computed from the smoothed image is lower. Additionally, smoothing the original image produces thicker edges, thus ringing artifacts may increase. Alternatively, higher contrast image with less severity of the mentioned problems can be obtained if the pixels with high noise levels and pixels around the edges are identified and are excluded from scaling.

In order to identify all or most problematic pixels, let's consider the following procedure which is explained using the hypothetical image shown in Figure 4(a). This image contains an edge between two smooth regions with some high level noise pixels indicated in bold font. If this image is first smoothed using a 3x3 averaging mask and then edges are detected using the Laplacian mask, the result in Figure 4(b) is obtained. In this image, it is clear how the response of some noise pixels is close to that of the pixels in the smooth regions they belong to. However, for noise pixels near the edge, their response is comparable to that of the pixels that are assumed to represent the edge. Also, note how many of the high responses are 2 pixels far from the edge due to smoothing and the double-edge effect of the Laplacian operator. Figure 4(c) shows a binary edge image that is obtained by thresholding the absolute edge image in Figure 4(b) using a threshold δ such that edge responses higher than δ (true edge pixels) are set to 1 while responses less than δ (noise and near edge pixels) are set 0. From this image we can see how some of the smooth regions and near-edge pixels are considered as edges. Most or all of the mistaken pixels can be removed by applying the morphological erosion operation [1,2] to eliminate isolated noise pixels and to thin the edge response. The erosion result is shown in Figure 4(d). It is clear in this image how edge response is almost completely lost while we still have false-positive edge pixels. Again this is directly tied with the fact that the Laplacian mask is used to compute the edge response.

Accordingly, to identify these problematic pixels, the filtering operation outlined earlier is modified to utilize a different edge operator to compute the edge response instead of using the Laplacian. For a smoothed image $\overline{f}(x,y)$, this operator is defined by

$$S(x,y) = \frac{1}{(2n+1)^2 - 1} \sum_{i=x-n}^{x+n} \sum_{k=y-n}^{y+n} \left| \overline{f}(x,y) - \overline{f}(x+i, y+k) \right| \quad , i \neq x \, , k \neq y \tag{7}$$

Basically, this equation computes the average of the absolute intensity difference between the pixel *(x,y)* and its adjacent pixels in a *(2n+1)x(2n+1)* neighborhood. Note how this operator is similar to the Laplacian in the sense that it computes the edge response through intensity differences. However, the weight for the center pixel is 1, which has the effect of reducing the Laplacian response of noisy pixels.

5	6	5	5	6	5	6
20	6	6	5	5	5	6
21	20	7	7	6	**30**	5
20	**10**	22	7	7	6	6
22	21	22	22	6	**30**	6
22	**10**	20	21	21	5	5
21	21	22	21	20	20	7

(a)

-9	-10	-11	-5	-7	-8	-7
12	1	-7	-12	11	7	7
12	5	-12	-14	0	**-2**	0
13	**15**	7	-3	5	0	6
-6	1	-2	10	-12	**-18**	-19
5	**6**	7	16	7	-5	-10
-1	0	-2	14	16	8	-7

(b)

1	1	1	1	1	1	1
1	0	1	1	1	1	1
1	1	1	1	0	0	0
1	1	1	0	1	0	1
1	0	0	1	1	1	1
1	1	1	1	1	1	1
0	0	0	1	1	1	1

(c)

1	0	1	1	1	1	1
0	0	0	1	0	0	0
1	0	1	0	0	0	0
1	0	0	0	0	0	0
0	0	0	0	1	0	1
0	0	0	1	1	1	1
0	0	0	0	1	1	1

(d)

Fig. 4. (a) Hypothetical image (b) edge image computed from the smoothed image using Laplacian operator (c) binary edge map (d) eroded binary edge map.

2	2	1	1	1	1	1
4	4	2	2	1	1	1
3	4	4	2	1	**0**	0
2	**2**	3	3	2	1	1
1	1	2	3	3	**3**	2
1	**1**	1	3	4	4	2
0	0	0	2	3	4	2

(a)

1	1	0	0	0	0	0
1	1	1	1	0	0	0
1	1	1	1	0	**0**	0
1	**1**	1	1	1	0	0
0	0	1	1	1	**1**	1
0	**0**	0	1	1	1	1
0	0	0	1	1	1	1

(b)

1	0	0	0	0	0	0
1	1	0	0	0	0	0
1	1	1	0	0	**0**	0
0	**0**	1	1	0	0	0
0	0	0	1	1	**0**	0
0	**0**	0	0	1	1	1
0	0	0	0	1	1	1

(c)

Fig. 5. (a) Edge image computed from the smoothed image using equation (7) (b) binary edge map (c) eroded binary edge map.

(a) (b) (c)

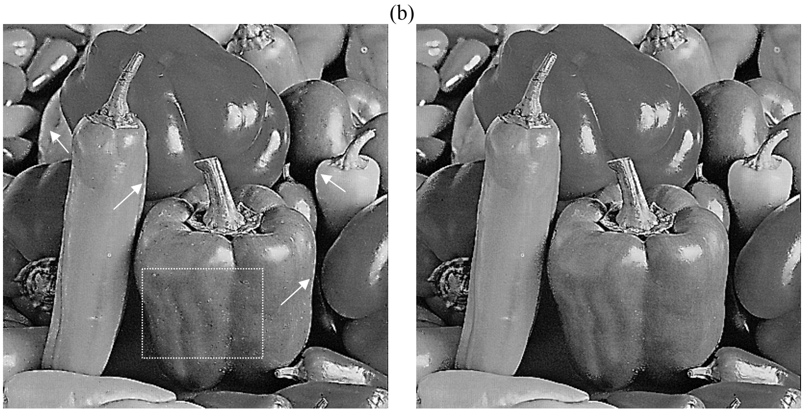

(d) (e)

Fig. 6. (a) Equalized edge image of Peppers image (b) filtered edge image using the Laplacian (c) filtered edge using the equation (7) (d) enhanced image using edge image in (b) (e) enhanced image using edge image in (c).

Additionally, the expression in (7) introduces some smoothing effect on the edge response since it computes the average difference between the center pixel and its neighbors. The result of applying this operation on the image in Figure 4(a) is shown in Figure 5(a). When compared with the Lapalcian edge response, it is obvious that edge responses obtained using equation (7) have more coherent values and are better localized. Also, the edge response within smooth regions is lower and coherent. Thus, levels of isolated noise pixels are reduced further. The corresponding binary edge image that is produced using a threshold δ is shown in Figure 5(b). Note how most of the isolated noise pixels have been eliminated and the pixels along the edge are preserved. However, the edge still contains many near edge pixels. As mentioned earlier, the erosion can be applied for further removal of isolated noise pixels and to thin the edge. This is shown Figure 5(c) which shows the binary edge map $R(x,y)$ that is supposed to

(a) Original (b) Unsharp masking (c) Ref. [15]

(d) Ref. [19] (e) Ref. [20] (f) Proposed

Fig. 7. Results for image *Boat.*

identify the edge pixels only. It is clear in this figure how the edge structure is preserved while isolated noise pixels are removed.

The edge map image *R(x,y)* obtained after erosion is assumed to identify the actual edge pixels, thus it can be used to filter the equalized edge image $E^w_{Scaled}(x,y)$ before it is added to the original image as given in (6). This should help in reducing noise amplification and ringing artifacts. This is achieved by using the equalized edge values for pixels that are identified as true edge pixels in $R(x,y)$ while for the remaining pixels the original edge value is used. In other words, the scaled edge image is modified such that

$$E^w_{Scaled}(x,y) = \begin{cases} E^w_{Scaled}(x,y) & , R(x,y)=1 \\ E^w(x,y) & , R(x,y)=0 \end{cases} \tag{8}$$

Considering real images, Figure 6 demonstrates the effectiveness of using the edge operator in (7) in the filtering operation of the scaled edge image and compares it with the result of using the Laplacian of the smoothed image. It is obvious in this figure how the noise level in smooth regions have significantly decreased after applying the filtering operation in both cases. However, edges obtained using equation (7) are more structured than those obtained when the filtering operation employs the Laplacian of the smoothed image as shown in figures 6(b) and 6(c). The enhanced images after filtering the scaled edge image in both cases are shown in Figures 6(d) and 6(e). Note how both images exhibit higher contrast when compared to the original image and less noise amplification and edge ringing when compared to the image in Figure 3(b) that was obtained using the proposed edge equalization technique without filtering. However, the image in Figure 6(e) has less ringing artifacts (examples are pointed to by white arrows) and lower noise amplification (an example is enclosed by the white rectangle) than the image in Figure 6(d).

B.3. Specification of Parameters

In general, the proposed technique is expected to increase the image contrast with less noise amplification and ringing artifacts given that the appropriate values for the four thresholds are specified. Typically, these values could be changed interactively until satisfactory result is obtained. The specification process should be done such that δ_2 and δ_3 are far from the origin to include most noise bins in $h_3(k)$, but not too far in order include weak edges in the scaling process. For δ_1 and δ_4, they should be far enough from the origin to obtain reasonable stretching for moderate edge values, but not too far in order to avoid ringing artifacts. Although it sounds simple, manual specification of the thresholds could be a time consuming job. Instead, the following approach is proposed to determine these thresholds automatically. The approach is defined based on an extensive experimentation on a large set of images.

For the thresholds δ_2 and δ_3, they are assumed to partition the edge image into smooth and edge regions. This can be simply achieved by applying any data clustering technique, such as K-means clustering and self-organizing

(a) Original (b) Unsharp masking (c) Ref. [15]
(d) Ref. [19] (e) Ref. [20] (f) Proposed

Fig. 8. Results for image *Cameraman.*

maps [29] on the edge image. In this paper, the K-means clustering algorithm is used because of its simplicity. Effectively, this algorithm attempt to group data points into clusters such that the intra-cluster similarity is minimized. Assuming that the edge histogram is symmetric, the K-means clustering algorithm is used to partition the absolute value of the edge image into two clusters; C_L and C_H, which represent the sets of low and high edge values, respectively. Consequently, we specify the two thresholds, δ_2 and δ_3, such that δ_3 is the center of C_L cluster and δ_2 is $-\delta_3$.

Actually, the logical procedure to apply the clustering algorithm should be to partition the edge image into three clusters; negative edge values, smooth edge values, and positive edge values, and then use some of the clusters statistics to specify the two thresholds. However, for many images, the K-means algorithm couldn't produce the three clusters as required. For example, the cluster that should include the true negative edge pixels sometimes had positive values for some images since the K-means algorithm does not employ any restrictions on the clustering process other than minimizing the intra-cluster similarity. On the other hand, clustering the absolute edge image into two clusters as described before guarantees that δ_2 is negative while δ_3 is positive.

Regarding the δ_1 and δ_4 thresholds, the straight forward approach could be to cluster the absolute edge image into three clusters instead of two. However, for all tested images this did not produce useful clusters due to the fact that most edge content is close to the origin, which results in low values for δ_1 and δ_4. Thus, the level of scaling is not high enough. Alternatively, these thresholds are specified using

$$\delta_1 = (\delta_2 + E^w_{\min})/2 \tag{9}$$

and

$$\delta_4 = (\delta_3 + E^w_{\max})/2 \tag{10}$$

Basically, the threshold δ_1 is the midpoint edge value between $E^w_{\min}$ and δ_2 while δ_4 is the midpoint edge value between δ_3 and $E^w_{\max}$.

Concerning the threshold δ that is used to compute the binary edge map *R(x,y)* is specified through clustering the edge response image *S(x,y)* into two clusters using the K-means clustering algorithm and then using the center of the cluster of low values as the values for δ. The assignment of the five thresholds using the approach presented here produced very satisfactory results for many test images.

III. Results & Discussion

In this section, the experimental results obtained using the proposed technique and the comparison with unsharp masking technique and the techniques described in [15], [19], and [20] are presented. The scale factor α for the unsharp masking technique is specified manually until the obtained contrast is visually comparable to that of the proposed technique. The results presented here include six 512x512 test images; *Boat, Cameraman, Toys, Cart, Lena,* and *Tank.* The thresholds δ, δ_1, δ_2, δ_3, and δ_4 used in the proposed technique are computed as discussed in Section II with the number of iterations for the K-means clustering algorithm set to 50. The smoothed image using in (7) is obtained using a 3x3 standard averaging mask.

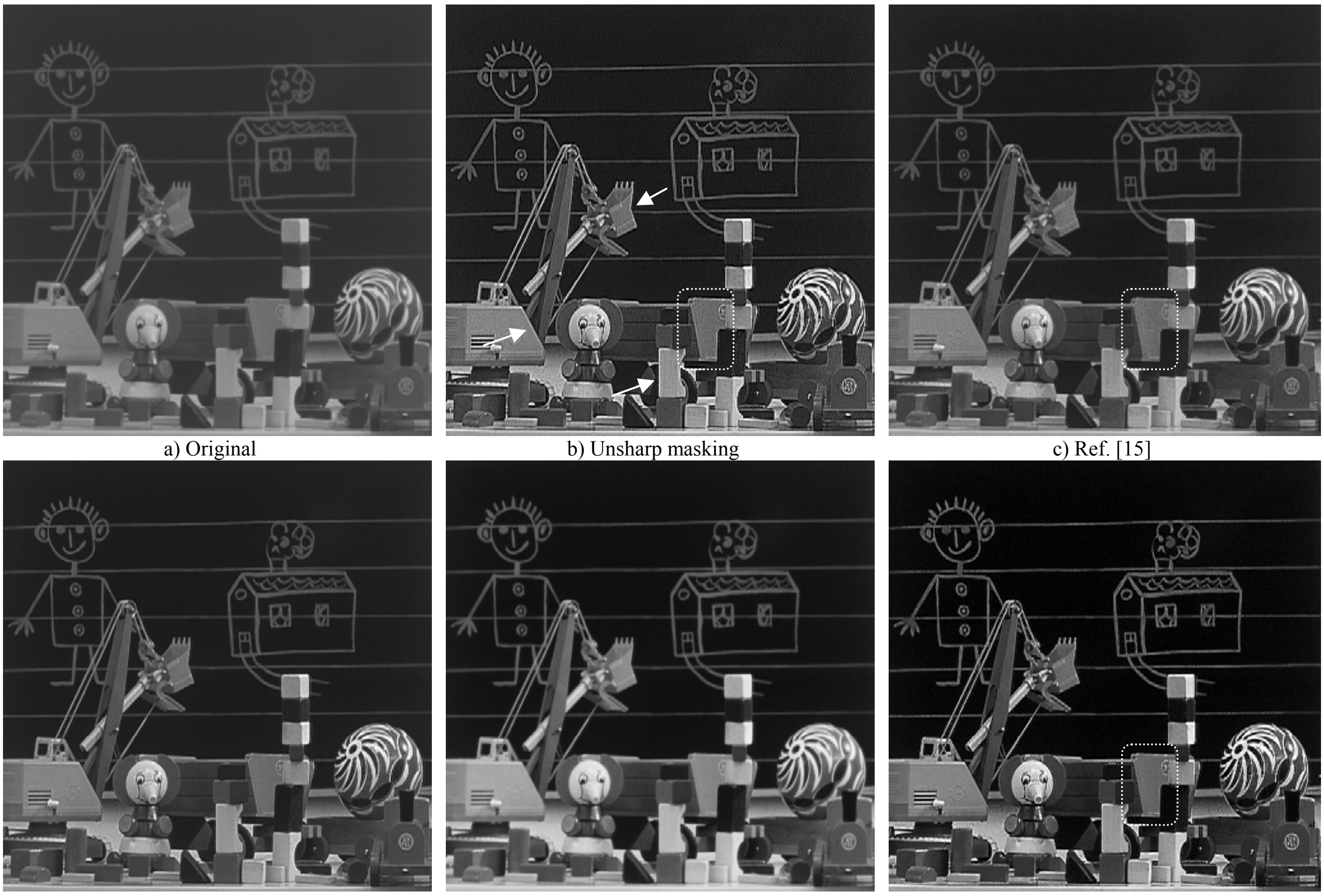

a) Original b) Unsharp masking c) Ref. [15]

(d) Ref. [19] (e) Ref. [20] (f) Proposed

Fig. 9. Results for image *Toys.*

In order to evaluate the results quantitatively, two contrast measures are used. The first one is the well-known benchmark image sharpness measure, the Tenegrad, is used [30]. The Tenegrad measure is based on gradient magnitude maximization and is considered one of the most robust and functionality accurate image quality measures [30]. The Tenegrad value is computed from the gradient at each pixel in the image where the partial derivatives are obtained by a high-pass filter such as Sobel operator. The Tenegrad (TEN) value for the whole image is computed using

$$TEN = \sum_x \sum_y G(x,y)\ ,\ \forall\ G(x,y) > \lambda \qquad (11)$$

where $G(x,y)$ is the gradient magnitude and λ is some threshold that is used to eliminate low edge responses which correspond to low levels of noise in the smooth regions in the image. In our experiments, λ is chosen to be the mean of the gradient magnitude values. The second contrast measure is the mean edge gray value [17], MEG, which is defined for a pixel *(x,y)* with *(2n+1)x(2n+1)* neighborhood by

$$MEG(x,y) = \frac{\sum_{k=x-n}^{x+n}\sum_{l=y-n}^{y+n}\Delta(k,l)f\left(k,l\right)}{\sum_{k=x-n}^{x+n}\sum_{l=y-n}^{y+n}\Delta(k,l)} \qquad (12)$$

with $\Delta(k,l)$ is the edge value computed using any edge operator such as Sobel or Roberts operators [1,2]. In the presented results, the average of MEG value of the entire *MxN* image

$$\overline{MEG} = \frac{1}{MN}\sum_{x=1}^{M}\sum_{y=1}^{N}\overline{E}(x,y) \qquad (13)$$

is reported. Generally, a high value of *MEG* for a certain image reflects better contrast.

The original test images and the enhanced images using different techniques and the proposed technique are shown in figures 7 through 12. In these figures, it is clear how the processed images are better contrasted than the original image. The best results in terms of enhancement level could be claimed for the unsharp masking technique. However, images obtained using unsharp masking exhibit severe ringing artifacts (examples are pointed to by the white arrows) and noise amplification (examples are enclosed in white rectangles). As mentioned earlier, this is due to the fact that enhancement in unsharp masking uses the actual edge values which may result in over-shooting and under-shooting in the intensity values in the enhanced image. Additionally, no special treatment for the noise that may exist in the image is provided. Such problems are less noticeable in the images produced by the proposed technique due to its capability of dealing with the causes of these problems through using the weighted edge values, partitioning the edge image to isolate noisy pixels, filtering of the scaled image. Nonetheless, the contrast of the images obtained using the proposed technique is quite comparable to that of the unsharp masking.

Regarding the comparison with the remaining techniques, it is obvious in the provided results how the proposed technique produces images with higher contrast. The technique in [15] resulted in noise amplification in smooth regions as indicated by the yellow rectangles in the figures. The Cheng et al. technique [19] produced images with no noise amplification and ringing artifacts as it uses four different homogeneity measures in the enhancement

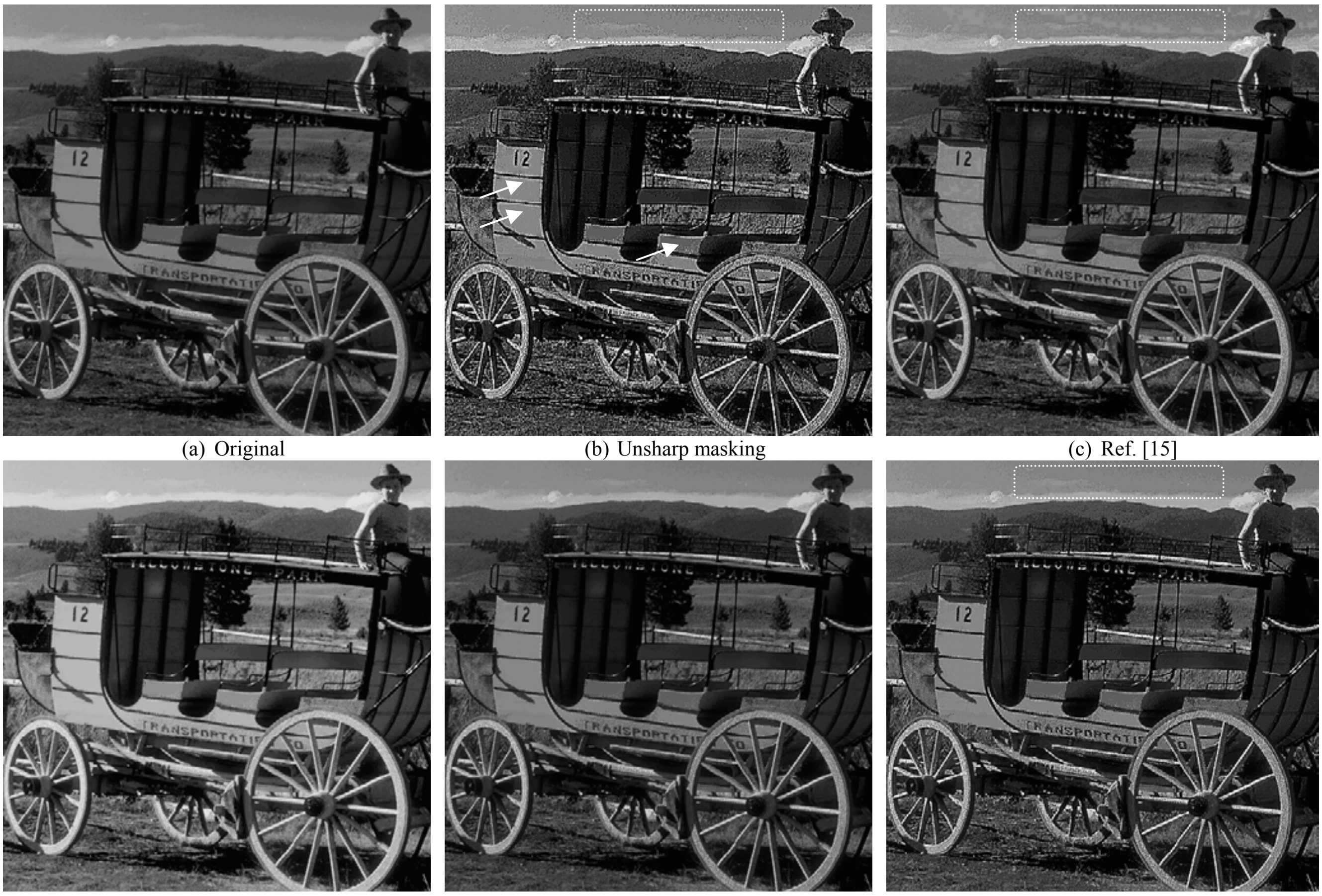

(a) Original (b) Unsharp masking (c) Ref. [15]

(d) Ref. [20] (e) Ref. [19] (f) Proposed

Fig. 10. Results for image *Cart.*

(a) Original (b) Unsharp masking (c) Ref. [15]

(d) Ref. [19] (e) Ref. [20] (f) Proposed

Fig. 11. Results for image *Lena.*

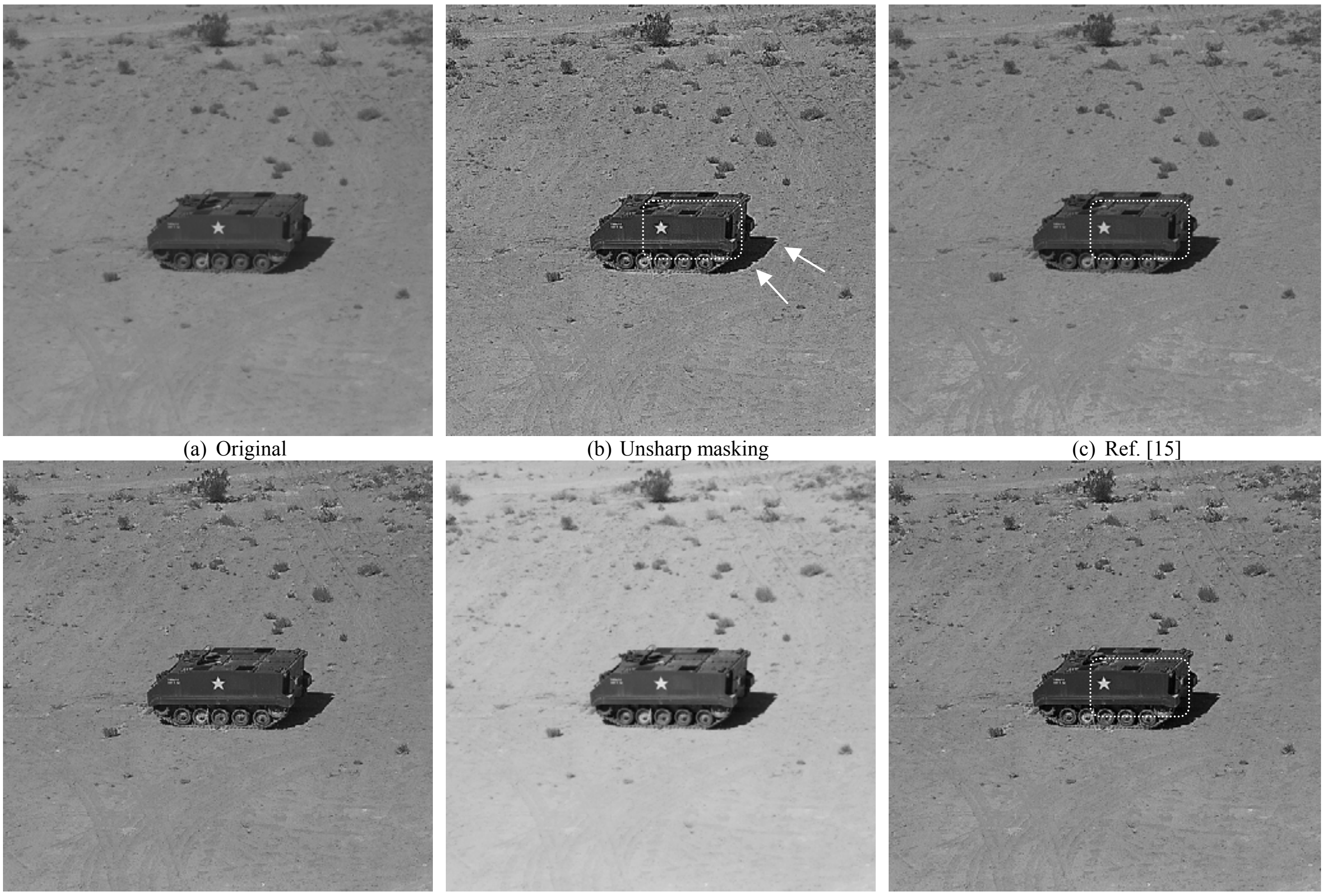

(a) Original (b) Unsharp masking (c) Ref. [15]

(d) Ref. [19] (e) Ref. [20] (f) Proposed

Fig. 12. Results for image *Tank*.

process. However, the level of enhancement is relatively low when compared to that of the proposed technique. This is due to the fact that the technique in [19] is very conservative in manipulating the contrast measure defined using the four homogeneity measures. Similarly, the technique in [20] exhibits lower levels of artifacts and lower contrast. Lower levels of contrast in this technique are due to the fact that the transformation function used for enhancement is applied globally, although it is derived based on local contrast measure.

Quantitatively, the TEN and MEG values for the four images before and after they are processed are listed in Tables II and III, respectively. Comparing these values of the original images with those of the processed images it is obvious how the processed images have higher values. This is good indication that the enhanced images for different techniques are of higher contrast and stronger edges, which is consistent with the visual evaluation. From the numbers given in Tables II and III, it is obvious how the proposed technique supersedes the techniques in [15], [19], and [20] as it has larger TEN and MEG values. However, these values are lower than those for the images processed by the unsharp masking technique. This is easily justifiable by the fact that the unsharp-masked images exhibit edge ringing artifacts due to overshooting and undershooting the intensity of many edge pixels. This makes the gradient response higher for such pixels, thus higher TEN and MEG values.

In terms of processing time, the average processing time for different techniques is listed in Table IV. These numbers are obtained by executing different techniques on a computer with 2.2 GHz Intel® Core 2 Duo and 3 GB of RAM. It is indisputable that the unsharp masking technique and the technique in [15] require lower time than other techniques due to their simplicity. From these numbers, it is obvious how the proposed technique requires moderate processing time when compared to the other techniques. The technique of [19] requires the longest time as it demands the computation of four homogeneity measures for each pixel in the image. Similarly, the technique in [20] is computationally expensive as it requires the computation of a set of expansion and anti-expansion forces for each intensity pair difference in the image.

In summary, experimental evaluation reveals the capability of the proposed technique in enhancing the image contrast and edge sharpness with less noise amplification and edge ringing artifacts with moderate processing requirements.

IV. Conclusion

In this paper, we presented a new technique for image contrast enhancement that is based on the popular unsharp masking technique. However, the proposed technique addresses the common problems associated with the unsharp masking. This is achieved through using an adapted version of the histogram equalization to scale the edge content in the image. Adaptation includes using weighted edge information, partitioning of the dynamic range of the edge histogram and equalizing the partitions that correspond to true edges only, as well as applying a filtering procedure on the scaled edge image before it is added to the original image. The effect of these resulted in better contrasted images with less noise amplification and ringing

TABLE II
TENEGRAD VALUES ($x10^7$) FOR THE ORIGINAL IMAGES AND THE RESULTS OBTAINED USING DIFFERENT TECHNIQUES

Image	Original	Unsharp Masking	Ref. [15]	Ref. [19]	Ref. [20]	Proposed
Boat	1.25	3.86	1.79	1.47	1.59	2.19
Cameraman	0.99	2.28	1.36	1.10	1.21	1.90
Toys	0.90	2.32	1.20	1.24	1.35	1.86
Cart	1.63	4.45	2.06	2.19	1.89	2.76
Lena	0.90	2.57	1.31	1.17	1.19	1.88
Tank	0.588	2.54	1.06	0.65	1.23	1.34

TABLE III
MEAN EDGE GRAY VALUES FOR THE ORIGINAL IMAGES AND THE RESULTS OBTAINED USING DIFFERENT TECHNIQUES

Image	Original	Unsharp Masking	Ref. [15]	Ref. [19]	Ref. [20]	Proposed
Boat	0.031	0.073	0.034	0.038	0.035	0.043
Cameraman	0.067	0.132	0.069	0.067	0.073	0.106
Toys	0.032	0.086	0.042	0.057	0.048	0.063
Cart	0.112	0.224	0.132	0.113	0.123	0.146
Lena	0.026	0.066	0.029	0.042	0.031	0.051
Tank	0.010939	0.034	0.015	0.012	0.018	0.023

Table IV
AVERAGE PROCESSING TIME IN SECONDS FOR DIFFERENT TECHNIQUES

Technique	Time (sec)
Unsharp masking	0.02
Ref. [15]	4.87
Ref. [19]	98.71
Ref. [20]	15.05
Proposed	10.93

artifacts when compared to the original unsharp and other enhancement techniques.

REFERENCES

[1] J.C. Russ, The Image Processing Handbook, CRC Press, 1995.

[2] R. Gonzalez, R.E. Woods, Digital Image Processing. Upper Saddle River, NJ, Prentice Hall, 2002.

[3] V.R. Vijaykumar, P.T. Vanathi, and P. Kanagasabapathy, “Fast and efficient algorithm to remove Gaussian noise in digital images,” IAENG International Journal of Computer Science, vol. 37, no. 1, February 2010.

[4] V.R. VijayKumar, S.Manikandan, D.Ebenezer, P.T.Vanathi and P.Kanagasabapathy, “High Density Impulse noise Removal in Color Images Using Median Controlled Adaptive Recursive Weighted Median Filter,” IAENG International Journal of Computer Science, vol. 34, no. 1, August 2007.

[5] A. Raji, A. Thaibaoui, E. Petit, P. Bunel, and G. Mimoun, “A gray-level transformation-based method for image enhancement,” *Pattern Recognition Letters*, vol. 19, no. 13, pp. 1207-1212, Nov. 1998.

[6] K. Iqbal, R. Abdul Salam, A. Osman and A. Talib, “Underwater image enhancement using an integrated colour model,” *IAENG International Journal of Computer Science*, vol. 34, no. 2, November 2007.

[7] E.H. Hall, “Almost uniform distribution for computer image enhancement,” *IEEE Transactions on Computers*, vol. 23, no. 2, pp. 207-208, Feb. 1974.

[8] D. Coltuc, P. Bolon, and J.M. Chassery, “ Exact histogram specification,” *IEEE Transactions on Image Processing*, vol. 15, no. 5, pp. 1143-1152, May 2006.

[9] W. Frei, “Image enhancement by histogram hyperbolization,” *Computer Vision, Graphics, and Image Processing*, vol. 6, no. 3 , pp. 286-294, June 1977.

[10] S. Yun, J. Kim, and S. Kim, “Contrast Enhancement using a weighted histogram equalization,” *In Proceedings of IEEE International Conference on Consumer Electronics*, Las Vegas, USA, January 2011.

[11] Z. Xu, H. R. Wu, X. Yu, and B. Qiu, “Colour image enhancement by virtual histogram approach,” *IEEE Transactions on Consumer Electronics*, vol. 56, no. 2, May 2010, pp. 704-712.

[12] S. Peleg, “Iterative histogram modification, 2,” *IEEE Transactions on Systems, Man, and Cybernetics*, vol. 8, no. 7, pp. 555-556, Nov. 1978.

[13] Z. Chen, B. Abidi, D. Page, and M. Abidi, “Gray-level grouping (GLG): an automatic method for optimized image contrast enhancement—part I: the basic method,” *IEEE Transactions on Image Processing*, vol. 15, no. 8, pp. 2290-2302, August 2006.

[14] S. Pal and R. King, “Image enhancement using fuzzy sets,” *Electronics Letters*, vol. 16, no. 10 , pp. 376-378, May 1980.

[15] S.C. Matz and R.J.P de Figueiredo, “A nonlinear image contrast sharpening approach based on Munsell’s scale,” *IEEE Transactions on Image Processing*, vol. 15, no. 4 , pp. 900-909, April 2006.

[16] R.M. Evans, The Perception of color, Wiley, New York, 1974.

[17] A. Beghdadi, “Design of an image distortion measure using spatial/spatial frequency analysis,” in *Proceedings of the IEEE First International Symposium on Control, Communications and Signal Processing*, 2004.

[18] M. Hanmandlu and D. Jha, “An optimal fuzzy system for color image enhancement,” *IEEE Transactions on Image Processing*, vol. 15, no. 10, October 2006, pp. 2956-2966.

[19] H.D. Cheng, M. Xue, and X.J. Shi, “Contrast enhancement based on a novel homogeneity measurement,” *Pattern Recognition*, vol. 36, no. , February 2003, pp. 2687 – 2697.

[20] T. Jen, B. Hsieh, and S. Wang, “Image contrast enhancement based on intensity-pair distribution,” in *Proceedings of IEEE International Conference on Image Processing*, Genoa, Italy, September 2005.

[21] L. Levi, “Unsharp masking and related image enhancement techniques,” *Computer Vision, Graphics, and Image Processing*, vol. 3, no. 2, June 1974, pp. 163-177.

[22] T.-L. Ji, M. K. Sundareshan, and H. Roehrig, “Adaptive image contrast enhancement based on human visual properties,” *IEEE Transactions on Medical Imaging,* vol. 13, no. 4, December 1994, pp. 573–586.

[23] V. Digalakis, D. G. Manolakis, V. K. Ingle, and A. K. Kok, “Automatic adaptive contrast enhancement for radiological imaging,” in *Proceedings of IEEE Int. Symp. Circuits Syst.,* Chicago, Illinois, May 1993.

[24] D. Chang and W. Wu, “Image contrast enhancement based on a histogram transformation of local standard deviation,” *IEEE Transactions on Medical Imaging*, vol. 17, no. 4, August 1998, pp. 518-531.

[25] S.-D Chen and A.R. Ramli, “Minimum mean brightness error bi-histogram equalization in contrast enhancement,” *IEEE Transactions on Consumer Electronics*, vol. 49, no. 4, Nov. 2003, pp. 1310-1319.
[26] C. Wang and Z. Ye, “Brightness preserving histogram equalization with maximum entropy: a variational perspective,” IEEE Transactions on Consumer Electronics, vol. 51, no. 4, November 2005, pp. 1326-1334.
[27] I. Jafar, and H. Ying, "Image contrast enhancement by constrained variational histogram equalization approach", pp. 143-148, in *Proceedings of the IEEE International Conference on Electro/Information Technology*, Chicago, May 2007.
[28] Y. Kim, “Contrast enhancement using brightness preserving bi-histogram equalization,” *IEEE Transactions on Consumer Electronics*, vol. 43, no. 1, Feb. 1997, pp. 1-8.
[29] J. C. Bezdek, J. Keller, R. Krisnapuram, and N. Pal, Fuzzy Models and Algorithms for Pattern Recognition and Image Processing (The Handbooks of Fuzzy Sets), Springer, New York, 2005.
[30] A. Buerkle, F. Schmoeckel, M. Kiefer, B. P. Amavasai, F. Caparrelli, A. N. Selvan, and J. R. Travis, “Vision-based closed-loop control of mobile microrobots for micro handling tasks,” in *Proceedings of SPIE*, vol. 4568, Microrobotics and Microassembly III, pp. 187–198, 2001.

Iyad F. Jafar received the B.S. degree in Electrical Engineering from The University of Jordan in 2001, the M.S. degree in Electrical Engineering from the Illinois Institute of Technology in 2004, and the Ph.D. degree in Computer Engineering from Wayne State University in 2008. He is currently working as an assistant professor in the Department of Computer Engineering at the University of Jordan. His research interests are in signal and image processing, pattern recognition, and computer networks.

Khalid A. Darabkh received his Ph.D. degree in Computer Engineering from University of Alabama in Huntsville, Alabama, USA in 2007. He is currently an assistant professor and the chair of Computer Engineering Department at the University of Jordan, Amman, Jordan. His main research interests include wireless and mobile communications, queuing theory, traffic management, multimedia systems and networking, congestion control architectures and resource allocation, parallel computing, and pattern recognition. Dr. Darabkh is a member of many honor societies such as Phi Kappa Phi, Tau Beta Pi, Eta Kappa Nu, and Sigma Xi.